Structure and Mechanical Properties of Low-Density Polyethylene/Spherical Silica Nanocomposites Prepared by Melt Mixing: The Joint Action of Silica's Size, Functionality, and Compatibilizer

Regina Jeziórska, Barbara Świerz-Motysia, Maria Zielecka, Agnieszka Szadkowska, Maciej Studziński

Department of Polymer Technology and Processing, Industrial Chemistry Research Institute, Rydygiera 8, Warsaw 02-372, Poland

Received 30 November 2011; accepted 30 November 2011
DOI 10.1002/app.36579
Published online in Wiley Online Library (wileyonlinelibrary.com).

ABSTRACT: Low-density polyethylene/spherical silica (LDPE/SGS) nanocomposites, containing 1, 2, and 6 wt % neat and modified (having amine functional groups) silica nanoparticles, were prepared by melt mixing using a twin-screw corotating extruder. To improve the dispersion degree of the nanoparticles, glicydyl methacrylate grafted ethylene/*n*-octene copolymer (EOR-*g*-GMA) containing 0.6 wt % GMA was used as a compatibilizer. It was observed that mechanical properties such as tensile strength, Young's modulus, and impact strength increase and are mainly affected by the loading and size of silica nanoparticles as well as by the EOR-*g*-GMA. The addition of modified silica and EOR-*g*-GMA resulted in a further enhancement of mechanical properties due to the improved interfacial adhesion. Storage and loss modulus values of prepared nanocomposites measured by dynamic-mechanical thermal analysis were sensitive to the microstructure of the nanocomposites. Higher storage and loss modulus are evidence that the nanocomposites became stiffer. By adding the modified silica and EOR-*g*-GMA further increase in storage and loss modulus were observed due to the better dispersion of silica nanoparticles and increased compatibility between silica and the LDPE matrix. Both permitted a much more efficient transfer of stress from the polymer matrix to the silica nanoparticles. The improved barrier properties of all nanocomposites can also be mentioned as a positive effect. © 2012 Wiley Periodicals, Inc. J Appl Polym Sci 000: 000–000, 2012

Key words: spherical silica nanoparticles; nanocomposites; low-density polyethylene; compatibilizer

INTRODUCTION

Nanosilica-filled polymer matrix composites have received considerable attention in the past few years. The potential of this new class of materials is outstanding, even small filler contents (<6 wt %) result in effective enhancement of the properties, unique and quite different from conventional composites. Mechanical properties enhancements, such as stiffness and toughness, dimensional, barrier and thermal properties as well as retardant improvements, with respect to the bulk polymer, are usually observed for this new class of materials.[1–7] These are typically attributed to the dramatic increase of the interfacial area between the filler and the polymeric matrix.[8–11] The dispersion degree of the filler greatly influences the improvement efficiency. Generally, the better the dispersion of fillers, the better the properties of the final nanocomposites. In fact, a poorly dispersed nanomaterial may reduce the mechanical properties.

Spherical silica (SGS) particles exhibit hydrophilicity and a very high surface energy due to their extremely high surface area per unit weight and the numerous silanol groups present on their surface due to their manufacturing process.[12] These characteristics lead to the formation of aggregates and particle–particle interactions between the filler particles in nonpolar liquids.[13] Thus in the case of a nonpolar polymer, such as low-density polyethylene (LDPE), the use of a compatibilizer is deemed necessary, such as glicydyl methacrylate grafted polyolefine elastomer (ethylene/*n*-octene copolymer [EOR-*g*-GMA]), to achieve a satisfactory dispersion of the filler in the polymer matrix. The compatibilizer should be miscible with the polyethylene matrix and it should include a certain amount of polar functional groups.[5,14,15] EOR modified with GMA fulfils these two requirements and to the best of our knowledge, has not been used in the preparation of polyethylene nanocomposites.

Correspondence to: R. Jeziórska (regina.jeziorska@ichp.pl).
Contract grant sponsor: National Centre of Research and Development; contract grant number: KB/146/13562/IT1-B/U/08.

In this study, to improve the dispersion degree of silica nanoparticles, modified nanosilica with surface amine reactive groups and EOR-*g*-GMA containing a 0.6 wt % GMA was used. It is believed that the surface silica amine functional groups of silica nanoparticles can react with the epoxy groups of EOR-*g*-GMA, leading to a finer dispersion of the individual silica nanoparticles in the LDPE matrix. The enhanced adhesion at the interface of the two materials, as a result of the mentioned reaction, has been investigated in this study.

Although there is no direct correlation between the filler particle size and the composites properties, a common observation is that it plays an important role due to the increase in the surface area of the inclusions and decrease in the interparticle distance with decreasing particle diameter. The aspect ratio of the inclusions also strongly influences the mechanical properties.[16] Generally, the elastic modulus increases while the other tensile properties such as strength and elongation at yield and break points decrease with increasing filler volume fraction.

The conclusion from our previous work concerning the study of polyamide 6/SGS nanocomposites, containing 0.5, 1, 2, and 4 wt % neat silica nanoparticles, was that the content of silica particles, as well as their size has a great impact on nanocomposites properties. Silica particles of 55 nm size have a higher tendency to produce agglomerates than bigger ones (100, 130 nm), which results in deterioration of mechanical properties (elongation and impact strength).[7]

Therefore, in this article, the effects of the silica loading, size, and its functionalities as well as EOR-*g*-GMA on the phase behavior, microstructure, and mechanical properties of LDPE nanocomposites were studied using scanning electron microscopy (SEM), dynamic-mechanical thermal analysis (DMTA), and tensile and impact testing. In addition, the ability of SGS loading and size to improve gas barrier properties of LDPE was also investigated.

EXPERIMENTAL

Materials

The LDPE used was Malen E FGNX 23D022 from Basell Orlen Polyolefines (Poland). LDPE has a melt flow rate (MFR) of 2.2 g/10 min (ISO 1133). Neat (SGS) and modified (having surface amine functional groups) SGS (SGS-A) nanoparticles synthesized according to the previously reported sol-gel process[7,12,17,18] were used as a nanofiller. In brief, silica was prepared as follows, ethyl alcohol (absolute, reagent grade), POCh S.A., Poland; aqueous ammonia (reagent grade, 25 wt %, $d = 0.91$ g/cm^3), POCh S.A., Poland; and distilled water were mixed to obtain the reaction mixture. The initial pH of the reaction mixture was measured with pH metre Schott Instruments LAB 850. All synthesis were carried out at room temperature (293 K). Tetraethoxysilane (TEOS; TES 28, technical grade), Wacker Chemie, Germany (distilled immediately before it was used for the preparation of nanoparticles), used as alkoxysilane precursor was added to the reaction mixture that was stirred with constant speed during 2 h. The reaction mixture containing TEOS : EtOH : H2O in the mole ratios 0.023 : 0.500 : 0.477 was used in the synthesis with the initial pH range of 10.4–11.3.

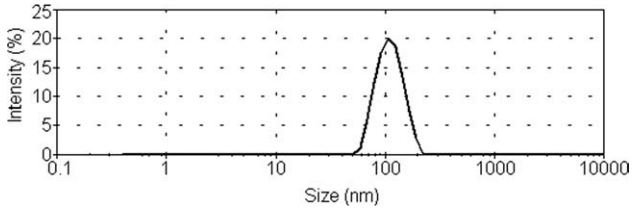

Figure 1 Size distribution of silica nanoparticles size 100 nm.

Modified silica nanoparticles were synthesized by adding drop by drop γ-aminopropylotriethoxysialne, Momentive Performance Materials (Columbus, Ohio), to the reaction mixture with further mixing during 1 h. The process of silica nanoparticles modification is given by the following reaction:

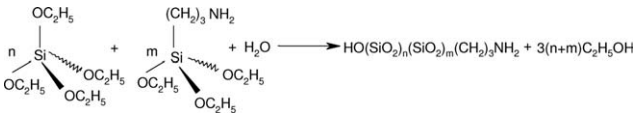

Nanosilica obtained from TEOS precursor was dried in an oven dryer for 2 h at 50–90°C or in a spray dryer. Particle size and particle size distribution in resulting sols were measured by photon correlation spectroscopy. The experiments were carried out with a Malvern apparatus (Zetasizer Nano ZS, Malvern, UK). The results were registered in the form of a curve of particle size distribution. The resulting peak analysis by intensity, volume, and number was performed. The developed synthesis method allows to obtain silica nanoparticles characterized by an almost uniform particle size, which is relative to the selection of the sol-gel process parameters, what is illustrated by the particle size distribution curve for nanosilica size of 100 nm (Fig. 1). The monomodal particle size distribution and very low polydispersity of particle size for both 60 and 100 nm particles were observed for homogeneous sols obtained by sol-gel process.

The SEM micrograph revealed spherical shape and uniform size of synthesized silica nanoparticles (Fig. 2). FTIR spectra of the nanosilica in the mid-IR range were recorded on PERKIN-ELMER System 2000 spectrometer both in KBr pellets in transmission mode and on KRS crystal in reflection mode.

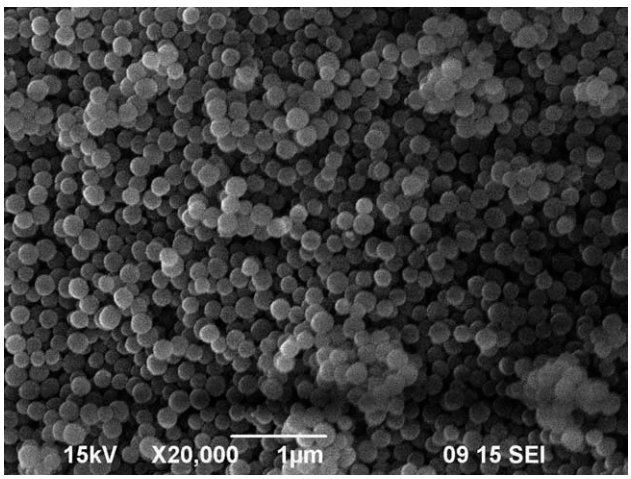

Figure 2 SEM image of nanosilica size 100 nm.

The IR spectra of the final silica nanoparticles did not reveal any presence of organic material, especially in the region of stretching vibrations C—H at 2900 cm^{-1}, thus confirming the completion of the hydrolysis reaction of Si—O—C bonds in alkoxysilane precursors.[17,19] The amine groups content was determined based on nitrogen content measurement by Kiejdahl method. The amine group content in all modified samples was 0.35 wt %. The average primary silica size was 60 and 100 nm. The characteristics of nanosilica fillers are presented in Table I.

The GMA was used for melt grafting onto polyolefine elastomer—EOR (Engage 8200, MFR 5.0 g/10 min at 190°C, from DuPont Dow Elastomers). Grafted copolymer (EOR-*g*-GMA), MFR 2.8 g/10 min at 190°C, containing 0.6 wt % GMA was prepared by melt blending according to the procedure published elsewhere[20,21] and used as a compatibilizer for nanocomposites at the concentration of 2 wt %.

Nanocomposites preparation

Nanocomposites containing 1, 2, and 6 wt % SGS nanoparticles were prepared by a two-step melt mixing in a Berstorff ZE-25x33D twin screw corotating extruder with $L/D = 33$ ($D = 25$ mm) according to the process published elsewhere.[22] Different screw elements along the screw worked to induce polymer melting and achieve a finer dispersion of the nanoparticles in the polymer melt.[23] The three mixing sections enhanced the compounding and also increased the residence time of the mixture in the barrel. The barrel pressure in these parts, as well as at the metering section before the die, could be increased. The extruder also had a vacuum degassing port to remove any moisture traces or other volatile products formed during compounding.

TABLE I
Characteristics of Nanosilica Fillers

Nanosilica	Size (nm)	Polydispersity	Amine groups content (wt %)
Neat silica	60	0.02	0
	100	0.03	0
Modified silica	60	0.03	0.35
	100	0.04	0.35

First, a masterbatch of 10 wt % of silica was prepared. Before the melt processing, this masterbach was dried for 3 h at 80°C. To prepare composites, the masterbach was compounded with pure LDPE or LDPE/EOR-*g*-GMA blend (98/2). All the materials were fed into the throat of the extruder using separate gravimetric feeders. Compounding was carried out using a screw speed of 300 rpm and also a temperature profile of 35, 145, 190, 190, 195, 195, 195, 195, and 215°C for the sequential heating zones, from the hopper to the die. The melt temperature and pressure were continuously recorded during compounding. After compounding, the material was extruded from the die, which had two cylindrical nozzles of 4 mm diameter, to produce cylindrical extrudates. These were immersed immediately in a cold-water bath (20°C) and pelletized with an adjustable rotating knife located behind the water bath into 5 mm pellets.

Measurements

The microstructure of silica nanoparticles and nanocomposites was examined by a JEOL JSM-6490LV SEM. Fourier transform infrared spectroscopy (FTIR) spectra were obtained using a Perkin-Elmer FTIR spectrometer, model Spectrum 1000. To collect the

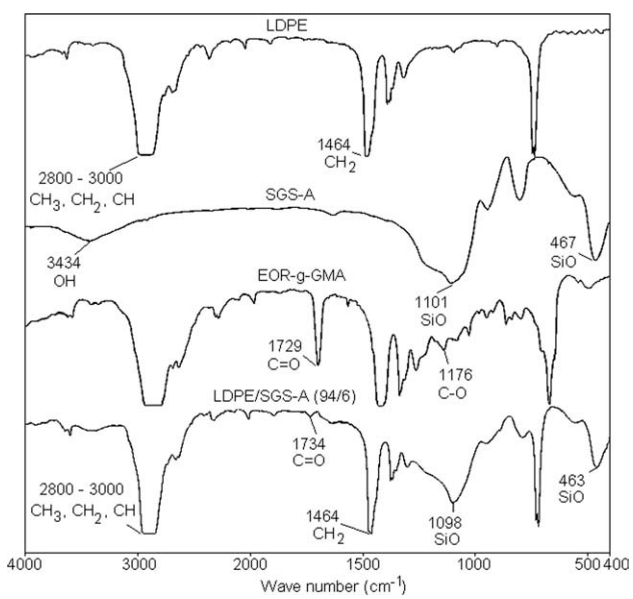

Figure 3 FTIR spectra of LDPE, SGS-A, EOR-*g*-GMA, and LDPE/SGS-A (94/6) nanocomposite containing 2 wt % EOR-*g*-GMA.

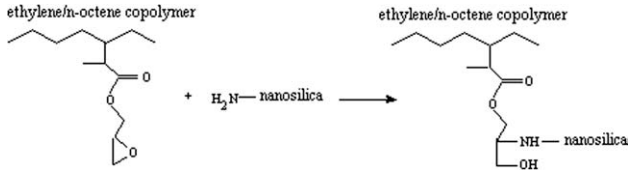

Scheme 1 Interaction between the epoxy groups of the EOR-*g*-GMA and the surface amine groups of silica nanoparticles.

spectra of the nanocomposites and polymers used, thin films were prepared in a hydraulic hot press. Nanosilica spectrum was taken using KBr pellets. The resolution for each spectrum was 2 cm^{-1} and the number of coadded scans was 64. The spectra presented were baseline corrected and converted to the absorbance mode. The dynamic mechanical analysis of samples was carried out using a dynamic mechanical analyzer, model Rheometrics RDS 2. The torsion method was used with a frequency of 1 Hz, a strain level of 0.1% in the temperature range of −150 to 100°C. The heating rate was 3°C/min. The testing was performed using rectangular bars measuring approximately $38 \times 10 \times 2$ mm^3. These were prepared by compression moulding, at a temperature of 190°C and pressure of 100 bar, for a time period of 5 min. The exact dimensions of each sample were measured before the scan. Dynamic viscosity was measured with Kinexus-PRO rheometer, Malvern, UK using the cone of 25 mm diameter as upper geometry and the plate of 55 mm diameter as lower geometry. All measurements were performed at 190°C. An Instron Series 4505, UK tensile tester that operated at a crosshead speed of 50 mm/min and at room temperature was used to measure the tensile properties of the composites according to ISO 527. Notched Charpy impact tests (Zwick 5102, Germany) were carried out in accordance with ISO 179 at room temperature. The specimens for the mechanical tests were prepared in an Arburg 420 M single screw injection machine (Allrounder 1000–250, Germany) containing five different heating zones. The temperatures of these were 175/185/200/205/195°C, from the feeding zone to the die, while the mould was cooled with water at 20°C. A minimum of 10 specimens for each LDPE/SGS composites were tested to estimate the precision of the reported data. Oxygen permeability tests of LDPE/SGS nanocomposites with various silica contents were performed with a MultiPerm apparatus (ExtraSolution, Italy). A press-molded thin film of uniform thickness (60 μm) was used for the test.

RESULTS AND DISCUSSION

FTIR analysis

Figure 3 shows the FTIR spectra of SGS-A, EOR-*g*-GMA, and LDPE/SGS-A nanocomposite of a 94/6 w/w composition containing 2 wt % EOR-*g*-GMA. In the spectrum of SGS-A there are two strong bands at 1101 and 467 cm^{-1} attributed to the Si—O groups and a broad peak with a maximum at 3434 cm^{-1} attributed to the surface hydroxyl groups. However, the peak of amine functional groups was not recorded, maybe due to the fact that silica contains only a very small amount of them (0.35 wt %). On the other hand, the most characteristic peaks of EOR-*g*-GMA, except those of EOR, are two peaks at a wave number of 1729 and 1176 cm^{-1} corresponding to the stretching vibration of C=O and C—O groups of GMA, respectively. In the spectrum of LDPE/SGS-A, nanocomposite of an 94/6 w/w composition containing 2 wt % EOR-*g*-GMA, the C—O groups of EOR-*g*-GMA are not recorded, maybe due to the very small amount that the nanocomposite contains (0.012 wt % GMA groups of the whole composition), as well as the amine peaks of SGS-A. Moreover a small peak at wave number 1734 cm^{-1} corresponding to the C=O groups from EOR-*g*-GMA and two peaks at a wave number of 1098 and 463 cm^{-1} that belong to the Si—O groups of silica were observed. The absorbance of C=O groups is moved to a higher wave number, but the peaks of

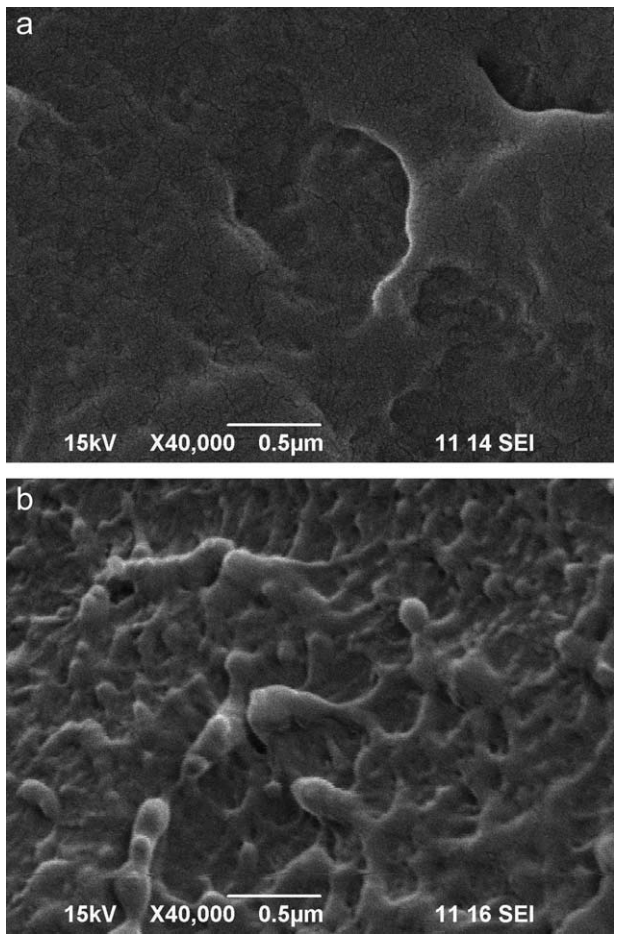

Figure 4 SEM images of: (a) LDPE; (b) LDPE/EOR-*g*-GMA 98/2.

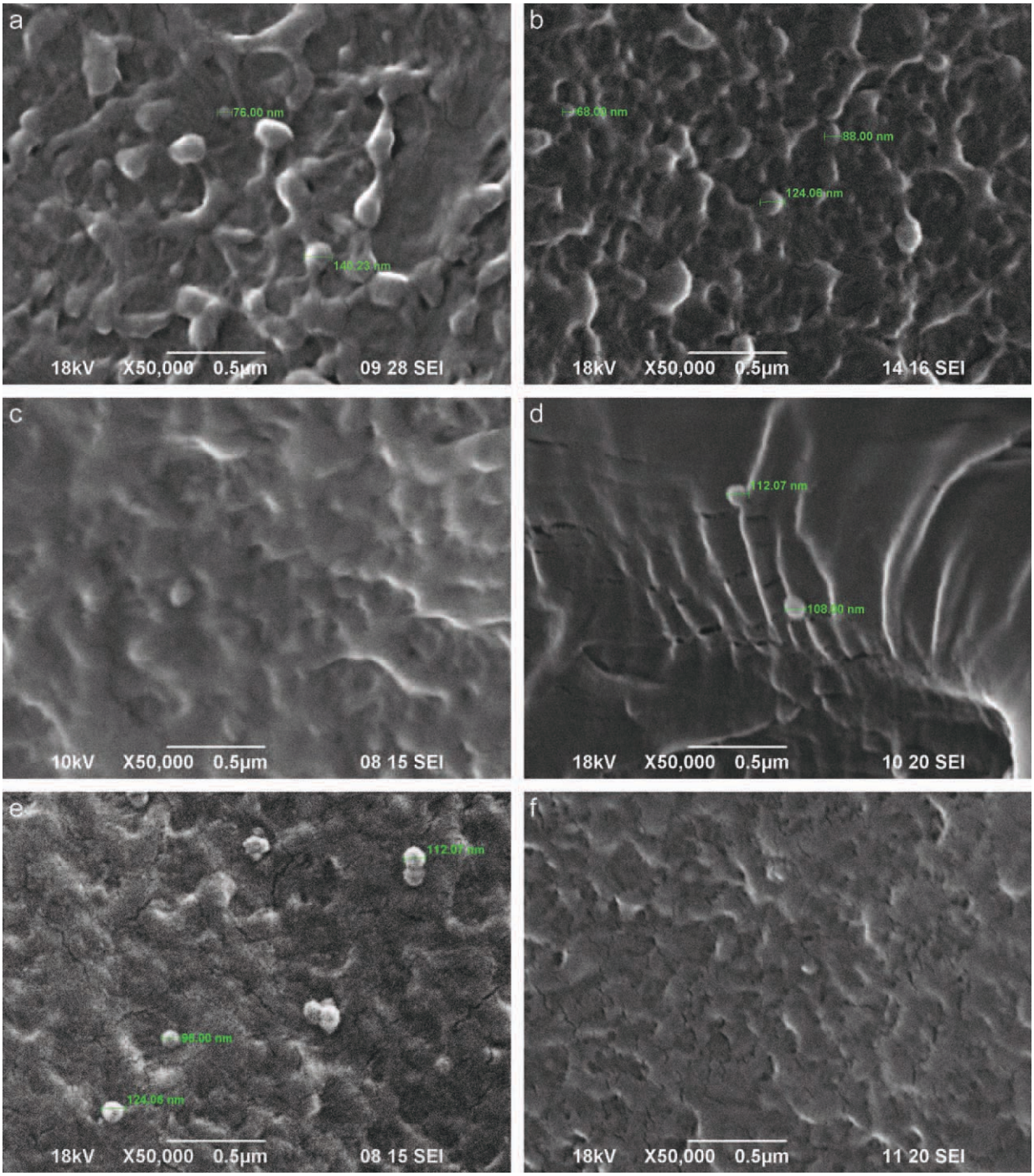

Figure 5 SEM images of nanocomposites: (a) LDPE with 1 wt % SGS; (b) LDPE/EOR-*g*-GMA 98/2 with 1 wt % SGS-A; (c) LDPE with 2 wt % SGS; (d) LDPE/EOR-*g*-GMA 98/2 with 2 wt % SGS-A; (e) LDPE with 6 wt % SGS; (f) LDPE/EOR-*g*-GMA 98/2 with 6 wt % SGS-A; silica size 100 nm. [Color figure can be viewed in the online issue, which is available at wileyonlinelibrary.com.]

Si—O groups are moved to a lower wave number compared with the ones of EOR-*g*-GMA and SGS-A, respectively. All discussed bands can be attributed to the mixture of components. However, these results are in good agreement with the findings of Bikiaris et al.,[15] who reported that the shift of the peaks that belong to the Si—O groups of silica in polypropylene nanocomposites containing 5 wt % maleic anhydride grafted polypropylene (PP-*g*-MA) to a lower wave number is maybe the result of the interactions that take place between the hydroxyl groups of silica and the maleic anhydride groups of PP-*g*-MA. On the basis of these findings, chemical and physical properties of the polyethylene nanocomposites containing 2 wt % EOR-*g*-GMA, the interactions between the amine groups of SGS-A and the epoxy groups of EOR-*g*-

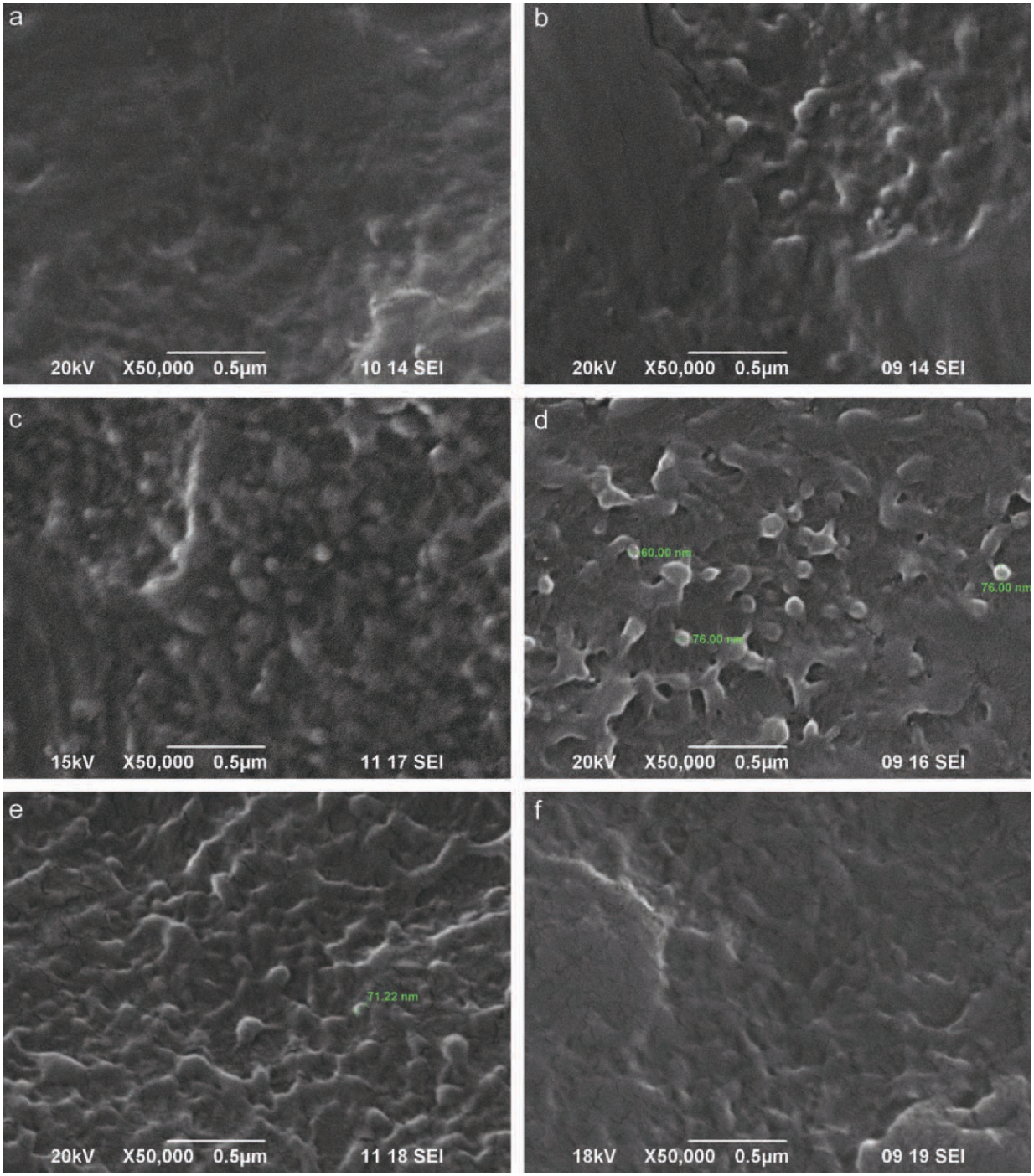

Figure 6 SEM images of nanocomposites: (a) LDPE with 1 wt % SGS; (b) LDPE/EOR-*g*-GMA 98/2 with 1 wt % SGS-A; (c) LDPE with 2 wt % SGS; (d) LDPE/EOR-*g*-GMA 98/2 with 2 wt % SGS-A; (e) LDPE with 6 wt % SGS; (f) LDPE/EOR-*g*-GMA 98/2 with 6 wt % SGS-A; silica size 60 nm. [Color figure can be viewed in the online issue, which is available at wileyonlinelibrary.com.]

GMA are possible and probably take place according to Scheme 1.

The effects of silica's size, functionality, and compatibilizer on the morphology and dispersion of nanosilica

Filler dispersion and adhesion with the polymer matrix are of great importance for improving the mechanical properties of composites. Fine control of the interface morphology of polymer nanocomposites is one of the most critical parameters to impart desired mechanical properties to such materials. To explain the behavior of the nanocomposites studied in this work, the surface of fractured specimens after injection moulding was examined with SEM. The image of the fractured surface of neat LDPE

TABLE II
Tensile and Impact Properties of LDPE and Composites for Silica Size 100 nm; Tensile Testing Speed 5 mm/min

SGS (wt %)	Tensile strength (MPa)	Elongation at max load (%)	Elongation at break (%)	Young's modulus (MPa)	Impact strength (kJ/m^2)
0	10.7 ± 0.2	84.4 ± 0.6	90.0 ± 0.3	270 ± 15	62 ± 2
1	12.9 ± 0.1	91.6 ± 1.2	94.9 ± 1.2	268 ± 14	68 ± 2
2	12.6 ± 0.2	88.9 ± 0.8	92.6 ± 0.3	260 ± 8	65 ± 2
6	12.3 ± 0.1	81.6 ± 1.4	85.7 ± 0.3	264 ± 10	62 ± 4

[Fig. 4(a)] shows relatively smooth surface. On the contrary, rough fracture surface is obtained for LDPE/EOR-*g*-GMA and nanocomposites [Figs. 4(b), 5, and 6] and the tendency toward the crack propagation is different. In the case of nanocomposites with neat silica and without EOR-*g*-GMA, rougher surface was observed at 1, 2, and 6 wt % of nanosilica. In contrast, nanocomposites with modified silica and 2 wt % EOR-*g*-GMA at similar nanosilica content show smoother fractured surface. Such a type of rough surface morphology can be related to the improvement in mechanical properties.[24] The SEM images showed that all the samples contain agglomerates. The tendency to form agglomerates increases with increasing silica content [Fig. 5(a,c,e)]. These results are in good agreement with the findings of Bikiaris et al.,[15] who reported that increasing the silica content in polypropylene nanocomposites leads to larger agglomerates.

Comparing nanocomposites containing neat nanosilica with the corresponding ones containing modified silica and EOR-*g*-GMA, the dispersion of individual silica nanoparticles in the LDPE matrix is finer [Fig. 5(c,d)]. The neat nanosilica tends to form large aggregates and agglomerates because of the formation of a hydrogen bond between the abundant hydroxyl groups and adsorbed water on their surface. This effect is more pronounced for higher concentrations of nanosilica.[7,15] After modification, most of hydroxyl groups have reacted and amine functional groups covered the nanosilica surface. Then, the surface has new more active centers, increasing the compatibility with the polar polymer matrix, and thus the adhesion between SGS-A and LDPE matrix is improved and the aggregation of the nanoparticles could be reduced [Fig. 5(e,f)]. The size of agglomerates will be further investigated by transmission electron microscopy and will be presented in the future study.

Figure 6 shows SEM images of LDPE/SGS and LDPE/EOR-*g*-GMA/SGS-A nanocomposites containing nanosilica size of 60 nm. It was found that silica nanoparticles are well distinguished in the LDPE matrix with and without the presence of the compatibilizer (2 wt % EOR-*g*-GMA). In all the samples, the silica particles are spherical in shape. It was also revealed that, at low concentrations (up to 1 wt %), neat silica exhibits a featureless morphology without discernable phase separation, which suggests homogenous structure. The reinforcement efficiency is related to the dispersion state of nanosilica in polyolefins. Therefore, the homogenous dispersion of silica will be effective in improving mechanical properties of low density polyethylene.

The effects of silica's size, functionality, and compatibilizer on the mechanical properties

To evaluate the reinforcing effect of nanoparticles on the LDPE matrix, mechanical properties during extension were measured. Because of the very high surface area of the nanoparticles in the LDPE/SGS nanocomposites, the applied stress is expected to be easily transferred from the matrix onto the silica particles resulting in an enhancement of the mechanical properties. Also, the EOR-*g*-GMA is expected to break up the large agglomerates of the nanoparticles into finer particles, resulting in an increase in their degree of dispersion in the polymeric matrix, increasing the interfacial adhesion. This can be achieved because the surface amine groups of the silica nanoparticles can react with the epoxy groups of the compatibilizer during processing, as shown in Scheme 1.

TABLE III
Tensile and Impact Properties of LDPE/EOR-*g*-GMA (98/2) and Composites for Silica Size 100 nm; Tensile Testing Speed 5 mm/min

SGS-A (wt %)	Tensile strength (MPa)	Elongation at max load (%)	Elongation at break (%)	Young's modulus (MPa)	Impact strength (kJ/m^2)
0	11.0 ± 0.2	83.0 ± 0.4	90.0 ± 0.3	250 ± 11	52 ± 2
1	13.0 ± 0.1	93.5 ± 0.8	98.2 ± 0.8	245 ± 7	69 ± 2
2	13.0 ± 0.1	89.8 ± 0.4	94.2 ± 0.3	246 ± 6	69 ± 2
6	13.0 ± 0.1	85.7 ± 0.7	89.6 ± 0.3	264 ± 8	67 ± 2

TABLE IV
Tensile and Impact Properties of LDPE Blends and Composites for Silica Size 60 nm; Tensile Testing Speed 5 mm/min

SGS (wt %)	Tensile strength (MPa)	Elongation at max load (%)	Elongation at break (%)	Young's modulus (MPa)	Impact strength (kJ/m^2)
0	10.7 ± 0.2	84.4 ± 0.6	90.0 ± 0.3	270 ± 15	62 ± 2
1	12.1 ± 0.1	75.0 ± 1.7	81.0 ± 1.7	263 ± 8	62 ± 2
2	12.4 ± 0.1	72.0 ± 0.8	78.0 ± 1.4	330 ± 6	60 ± 2
6	12.2 ± 0.1	66.0 ± 2.3	72.0 ± 2.3	322 ± 7	63 ± 3

In Tables II and III, the tensile properties for the LDPE/SGS nanocomposites containing neat SGS and LDPE/EOR-*g*-GMA (98/2) nanocomposites with modified SGS-A (having amine functional groups) with particle size of 100 nm are presented as a function of silica content. Comparing the nanocomposites, a gradual increase in tensile strength is observed for neat SGS with particle size of 100 nm contents up to 1 wt %, reaching 20% in comparison to the initial value. For silica concentrations higher than 1 wt %, a small decrease is observed. This reduction in tensile strength observed for silica concentrations higher than 1 wt % should be associated with the extended aggregation of silica nanoparticles, which increased with increasing silica amounts, as observed in SEM micrographs discussed earlier. This is in agreement with a similar deterioration of mechanical properties reported for PP/fumed silica nanocomposites.[15]

For composites containing greater amounts of silica nanoparticles, up to 6 wt %, an enhancement of tensile strength can be observed when silica with amine functionality and EOR-*g*-GMA are used.

A similar variation to that discussed above can be seen in tensile strength for the nanocomposites containing silica with particle size of 60 nm (Tables IV and V). A small increase of 12% can be seen, compared to the initial value, for neat silica. This effect is independent of the percentage of silica. Further enhancement of 18% in tensile strength can be obtained for modified silica and the EOR-*g*-GMA used as a compatibilizer at the concentration of 1 and 2 wt %, respectively. Above 1 wt % filler concentration there is a linear decrease. This decrease is also related to the extended agglomeration of silica nanoparticles, which, as was mentioned earlier, increased with greater silica content. Concerning the effect of silica size, it appears that tensile strength of the LDPE nanocomposites with silica size of 60 nm is a little bit lower than that containing silica size of 100 nm.

Comparing all composites (Tables II–V), it is obvious that increasing the loading of silica induces a small, almost linear, decrease in elongation at yield and break points of the sample. The decrease reaches up to 8%, compared to neat LDPE, for the sample containing 6 wt % SGS size of 60 nm. However, the presence of neat silica size of 100 nm up to 2 wt % improves elongation of the polyethylene composites. On the other hand, the composites obtained with neat silica size of 60 nm exhibit lower elongation compared with the 100 nm ones and to neat LDPE. The addition of modified silica and EOR-*g*-GMA has a positive effect on the elongation at break, namely at higher silica concentrations. This improvement in elongation for composites obtained with modified silica and the compatibilizer should be associated with smaller agglomerations of silica nanoparticles, which usually act as stress concentrators of failure points of the material. It seems that, with the addition of compatibilizer, which results in a better dispersion of the nanoparticles and greater adhesion between them and the matrix, the interaction between the particles and the matrix is greater, making it easier for properties to be transferred between the two materials. The silica nanoparticles, which are rigid and have almost no elongation, retain this property in the final composite material. As a result they inhibit the elongation of the nanocomposite, making it less ductile. However, the observed reduction in elongation at break does not affect the properties of nanocomposites, and they can be still used even for film production.

TABLE V
Tensile and Impact Properties of LDPE/EOR-*g*-GMA (98/2) Composites for Silica Size 60 nm; Tensile Testing Speed 5 mm/min

SGS-A (wt %)	Tensile strength (MPa)	Elongation at max load (%)	Elongation at break (%)	Young's modulus (MPa)	Impact strength (kJ/m^2)
0	11.0 ± 0.2	83.0 ± 0.4	90.0 ± 0.3	250 ± 11	52 ± 2
1	13.0 ± 0.1	77.5 ± 0.8	82.2 ± 0.7	260 ± 5	67 ± 2
2	12.0 ± 0.1	75.8 ± 0.6	81.2 ± 0.8	359 ± 7	64 ± 2
6	12.0 ± 0.1	68.7 ± 1.6	73.6 ± 1.5	375 ± 7	65 ± 2

In the case of Young's modulus, the results are impressive and higher than those produced via *in situ* polymerization in the literature.[24] The addition of modified silica with particle size of 60 nm and the compatibilizer, which improves the dispersion degree of nanoparticles and increases adhesion between them and the polymer matrix, just as in the previous cases, results in a great improvement of Young's modulus, by almost 40 and 50% regarded to neat LDPE and LDPE/EOR-*g*-GMA (98/2), respectively. Comparing the effect of the silica size, it appears that Young's modulus of the samples with silica size of 60 nm (neat and modified) and the compatibilizer is significantly higher than that in the corresponding samples obtained with silica size of 100 nm. This is further proof that mechanical properties of nanocomposites could be better if nanoparticles were more finely dispersed into the polymeric matrix, without the occurrence of aggregates.

Moreover, an increase of 5–10% in notched Charpy impact strength is achieved in the LDPE/SGS nanocomposites containing neat silica with particles size of 100. The maximum was observed at silica loading of 1 wt %. The decrease in impact strength at higher silica contents can be explained due to the aggregation of silica nanoparticles at higher concentrations. The addition of amine functionalized silica and the EOR-*g*-GMA has a positive effect on the impact strength, just like it does for the other mechanical properties.

The degree of effectiveness of the nanoparticles, however, depends not only on the filler loading, its functionality and the compatibilizer used but also on the silica size. The impact strength of the samples with silica size of 60 nm (neat and modified) and the compatibilizer is slightly lower than that in the corresponding samples obtained with silica size of 100 nm. This is likely due to the higher stiffness.

Dynamic-mechanical properties

DMTA can provide reliable information about the relaxation behavior of the examined materials. To evaluate the effect of SGS nanoparticles on the LDPE matrix, thermomechanical properties were measured. Because of the very high surface area of the nanoparticles in the LDPE/SGS nanocomposites, the applied stresses are expected to be easily transferred from the matrix onto the silica particles, resulting in an enhancement of the mechanical properties. Also, the compatibilizer can break up large agglomerates of the nanoparticles into finer particles, resulting in an increase of their degree of dispersion in the polymeric matrix, increasing the interfacial adhesion. This is accomplished because, during the melt blending of the nanocomposites, the amine functional groups of the silica nanoparticles could react with epoxy functional groups of EOR-*g*-GMA. Finer dispersion of nanoparticles could lead to a further enhancement of thermomechanical properties. Plots of storage (G′), loss modulus (G″), and loss tangent (tan δ) as a function of temperature at 1 Hz for LDPE, LDPE/EOR-*g*-GMA, and the composites with different contents of silica, size of 60 nm, are presented in Figure 7; the storage modulus at room temperature and temperatures of relaxations α, β, and γ are shown in Tables VI and VII.

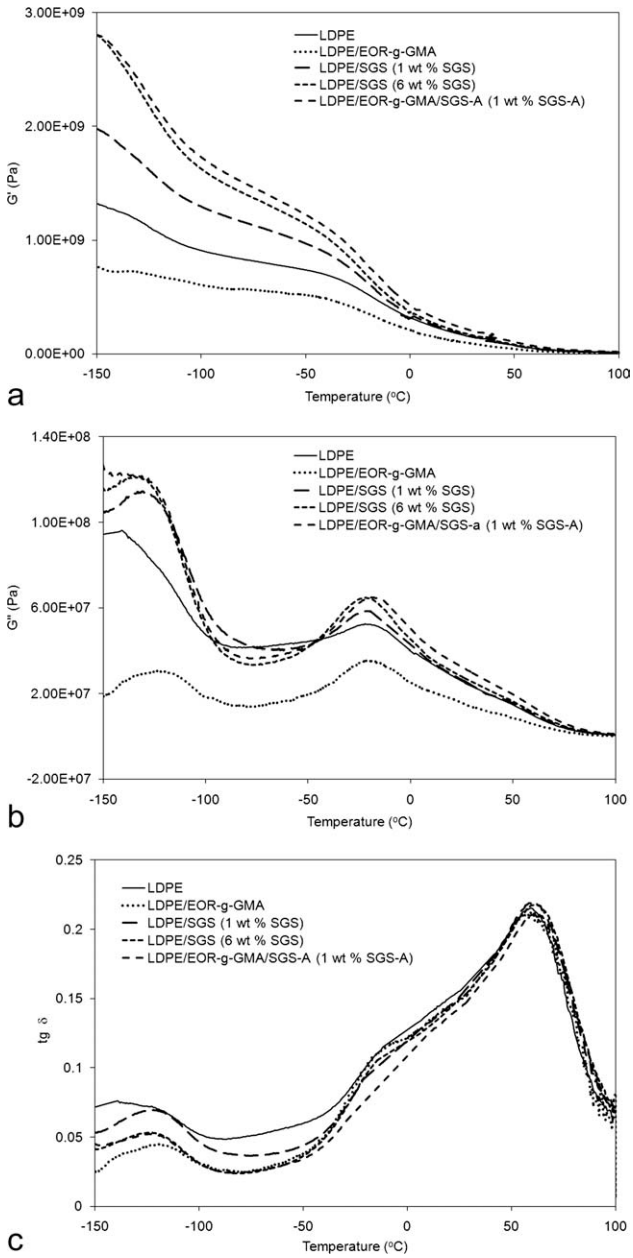

Figure 7 Dynamic mechanical relaxation behavior versus temperature of LDPE, LDPE/EOR-*g*-GMA and the nanocomposites at frequency of 1 Hz: (a) G′; (b) G″ (c) tan δ; silica size 60 nm.

The tan δ and loss modulus (G″) maximums show three (γ, β, and α) and two relaxations (γ and β),

TABLE VI
DMTA Results for LDPE, LDPE/EOR-*g*-GMA (98/2), and the Nanocomposites; Silica Size 60 nm

Sample	SGS (wt %)	Storage modulus (Pa) at 25°C	Loss modulus (peak position) (°C)		Loss modulus (peak high) (Pa)	
			T_γ	T_β	T_γ	T_β
LDPE	0	1.6×10^8	−140	−20	9.6×10^7	5.2×10^7
LDPE/EOR-*g*-GMA	0	1.1×10^8	−123	−23	3.1×10^7	3.5×10^7
LDPE/SGS	1	1.8×10^8	−130	−20	1.1×10^8	5.8×10^7
LDPE/EOR-*g*-GMA/SGS-A	1	1.9×10^8	−135	−19	1.2×10^8	6.5×10^7
LDPE/SGS	6	2.2×10^8	−132	−19	1.2×10^8	6.5×10^7

which take place in the specimens in order of decreasing temperature, respectively. These are accompanied by a pronounced decrease of the storage modulus.

The γ-relaxation has been associated with a single relaxation process, predominantly of amorphous origin. This relaxation is typical of the joint movements of chains containing three or more methylene groups (units) in the main chain.[25,26] The γ-relaxation appears as a maximum at −129°C for the LDPE and around −125°C for the nanocomposites in tan δ and at significantly lower temperatures in loss modulus, with a corresponding decrease in storage modulus. This is a clear effect of silica content, its functionality and the used compatibilizer on the breadth and on the location of the relaxation; this process is shifted to higher temperatures in the presence of neat silica and modified silica with EOR-*g*-GMA, as a consequence of higher crystallinity. Moreover, the γ-relaxation peak's intensity increases for the nanocomposites as a function of neat nanosilica. The addition of modified silica and the compatibilizer further increases the intensity of this peak as compared to unmodified silica at the same content. On the other hand, the γ-relaxation peak's intensity decreases for LDPE/EOR-*g*-GMA as a consequence of reduced crystallinity.

The α-relaxation has been defined as the reorientation of molecules within the crystals.[27] It was reported[25] that there is a relation between crystal thickness and intensity of the α-relaxation, and that this process is affected by the chain mobility of the crystals. Therefore, chain mobility occurs at higher temperatures as crystallite thickness increases. The position and intensity of the α-relaxation maximum is usually connected with crystal thickness and crystallinity level, respectively.[28] There is no evidence in these samples of the α-relaxation in loss modulus. On the other hand, the α-relaxation shows a clear maximum in tan δ. In the LDPE and LDPE/EOR-*g*-GMA samples, the α-relaxation appears centered at 57°C and in the LDPE/SGS nanocomposites, at 58°C when the neat silica content is 1wt % and 59°C when the neat silica content is 6 wt % and modified silica and compatibilizer are used. Simultaneously, the β-relaxation can be observed as a weak shoulder in the α relaxation in tan δ and as a clear maximum in loss modulus and its temperature does not vary much (Fig. 7). However, the β-relaxation process usually appears in the high molecular weight polyethylene at temperatures around −20°C, it rarely and weakly exists, in some samples of linear polyethylene.[28–30] Some authors have concluded that the β-relaxation results from motions of chain units in the interfacial region[28] whereas others attributed this process to the glass transition.[31]

The storage and loss modulus of the composites were higher than corresponding LDPE and LDPE/

TABLE VII
DMTA Results for LDPE, LDPE/EOR-*g*-GMA (98/2), and the Nanocomposites; Silica Size 60 nm

Sample	SGS (wt %)	Loss tangent (peak position) (°C)		
		T_γ	T_β	T_α
LDPE	0	−129	−13	57
LDPE/EOR-*g*-GMA	0	−123	−15	57
LDPE/SGS	1	−126	−23	58
LDPE/EOR-*g*-GMA/SGS-A	1	−125	–	59
LDPE/SGS	6	−127	−16	59

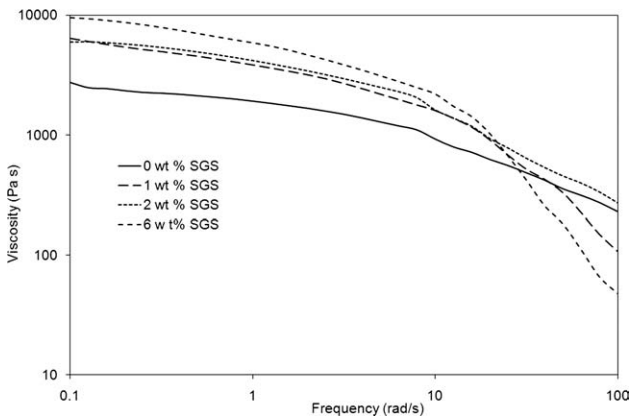

Figure 8 Viscosity versus frequency of LDPE and the LDPE/SGS nanocomposites with different silica contents; silica size 60 nm.

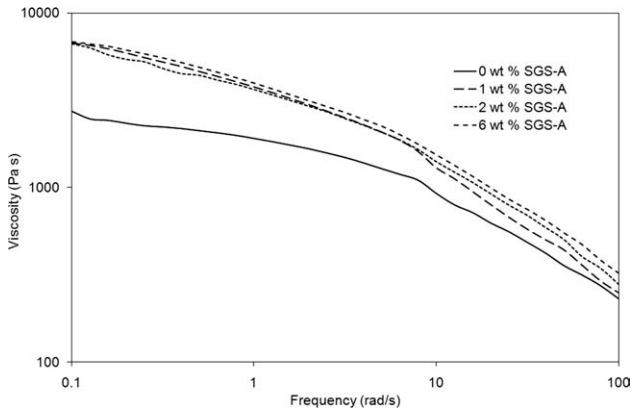

Figure 9 Viscosity versus frequency of LDPE and the LDPE/EOR-*g*-GMA/SGS-A nanocomposites with different silica contents; silica size 60 nm.

EOR-*g*-GMA, particularly at lower temperatures, that is, from −100 to 0°C, while above 0°C the differences between the various modulus became minimal. Moreover, the storage and loss modulus of the composites increased with increasing SGS content. Silica could affect the LPDE chain through the active centers formed by silanol or amine functional groups through the reaction with epoxy functional groups of EOR-*g*-GMA and hinder the chain motion of LDPE, which would improve the modulus. As a result of these changes, the storage modulus of the interface is higher than that of the free part.

The change in the viscosity (η*) of LDPE and the nanocomposites are shown in Figures 8 and 9. It is observed from Figures 8 and 9 that the viscosity decreases with increased frequency. This is due to the strong shear thinning behavior of the polymer nanocomposite and its pristine equivalent at the melted state. The viscosity of the nanocomposites is higher than neat LDPE. At 1 rad/s, the viscosity of LDPE/SGS containing 6 wt % SGS is 52% higher than the viscosity of LDPE/SGS containing 1 wt % SGS whereas it is over 200% higher compared to neat LDPE (Table VIII). The increment of melt viscosity of the nanocomposites is attributed to the strong interaction of silica and polymer matrix. However, the viscosity of the composites containing modified silica and the compatibilizer is lower than the ones with neat silica. This is due to the fact that

TABLE VIII
Viscosity Results for LDPE and the Nanocomposites with and without EOR-*g*-GMA

	Viscosity at 1 rad/s (Pa s)	
SGS (wt %)	0 wt % EOR-*g*-GMA	2 wt % EOR-GMA
0	1912	1912
1	3864	3783
2	4183	3664
6	5858	3997

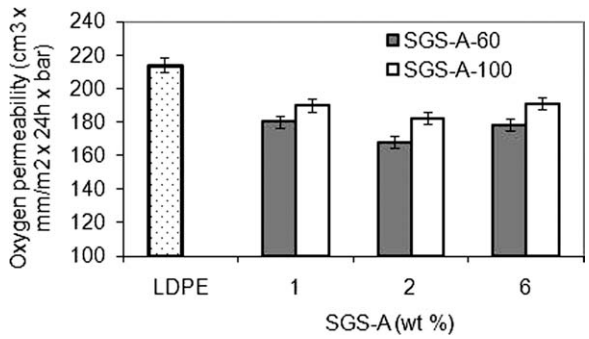

Figure 10 Oxygen permeability of LDPE and the LDPE/EOR-*g*-GMA/SGS-A nanocomposites with different silica sizes and contents.

the LDPE/EOR-*g*-GMA/SGS-A composites contain much lower molecular weight and significantly less viscous compatibilizer (EOR-*g*-GMA) compared to the LDPE/SGS composites.

The effects of silica's size, functionality and compatibilizer on the barrier properties

Introducing nanosilica into polyethylene also improved the gas barrier properties. Figure 10 shows the oxygen permeability of the nanocomposites films. Generally, with increasing silica content, the barrier properties also increase as a result of the tortuous path created by silica spherical nanoparticles.[1] However, nanocomposites with silica particles of 60 nm size have lower oxygen permeability than the ones with silica particles of 100 nm. Loading 2 wt % SGS-A particles of 60 nm size improved the barrier properties by about 23% compared to neat LDPE.

CONCLUSIONS

It was revealed that the content and size of nanosilica as well as its functionality and the used compatibilizer (EOR-*g*-GMA) affected the dispersion degree of the nanoparticles. From SEM, it was found that the addition of modified silica and EOR-*g*-GMA as a compatibilizer improves the adhesion between the LDPE matrix and SGS-A nanoparticles, due to the possible interactions between the reactive groups.

The nanocomposites obtained with a few weight percent of silica nanoparticles (1−6 wt %) showed significant improvement in tensile strength, Young's modulus, and impact strength, so silica nanoparticles act as reinforcing agents. When the concentration is above 1−2 wt %, mechanical properties decrease. This behavior is attributed to large aggregates of silica nanoparticles that are formed during the processing. The addition of modified silica as well as EOR-*g*-GMA results in a finer dispersion of individual silica nanoparticles in the LDPE matrix as verified by SEM, inducing a further enhancement in mechanical properties.

Thermomechanical measurements confirmed these observations, showing an enhancement of the storage and loss modulus, which increases with increasing silica contents. It is particularly interesting to point out that addition of modified silica and the compatibilizer further improved storage and loss modulus. The presence of silica nanoparticles also enhances the viscosity and barrier properties of the polyethylene composites.

The authors are grateful to Mrs. Irena Leszczyńska from Industrial Chemistry Research Institute (Poland) for FTIR analyses.

References

1. Vladimirov, V.; Betchev, C.; Vassiliou, A.; Papageorgiou, G.; Bikiaris, D. Compos Sci Technol 2006, 66, 2935.
2. Kontou, E.; Niaounakis, M. Polymer 2006, 47, 1267.
3. Liu, Y.; Kontopoulou, M. Polymer 2006, 47, 7731.
4. Chen, J. H.; Rong, M. Z.; Ruan, W. H.; Zhang, M. Q. Compos Sci Technol 2009, 69, 252.
5. Barus, S.; Zanetti, M.; Lazzari, M.; Costa, L. Polymer 2009, 50, 2595.
6. Ji, Q.; Wang, X.; Zhang, Y.; Kong, Q.; Xia, Y. Compos A 2009, 40, 878.
7. Jeziórska, R.; Zielecka, M.; Świerz-Motysia, B.; Studziński, M. Polimery 2009, 54, 727.
8. Song, G. J. Mater Rep 1996, 4, 57.
9. Dorigato, A.; Pegoretti, A.; Penati, A. eXPRESS Polym Lett 2010, 4, 115.
10. Osman, M. A.; Atallah, A. Polymer 2005, 46, 9476.
11. Osman, M. A.; Atallah, A. Polymer 2006, 47, 2357.
12. Zielecka, M.; Bajdor, K.; Szulc, A.; Bujnowska, E.; Cyruchin, K. Pol. Pat. 198 188, June 30, 2008.
13. Barthel, H. Colloid Surf A 1995, 101, 217.
14. Lee, J.-H.; Jung, D.; Hong, C.-E.; Rhee, K. Y.; Advani, S. G. Compos Sci Technol 2005, 65, 1996.
15. Bikiaris, D. B.; Vassiliou, A.; Pavlidou, E.; Karayannidis, G. B. Eur Polym J 2005, 41, 1965.
16. Osman, M. A.; Atallah, A.; Muller, M.; Suter, U. W. Polymer 2001, 42, 6545.
17. Zielecka M.; Bajdor K.; Bujnowska E.; Cyruchin K. Przemysł Chemiczny 2007, 86, 305.
18. Ryszkowska, J.; Waśniewski, B.; Pytel, A.; Zielecka, M. Polimery 2009, 54, 737.
19. Zielecka M.; Bujnowska E.; Kępska B.; Wenda M.; Piotrowska M. Progress in Organic Coatings, 2011, 72, 193–201, doi:10.1016/j.porgcoat.2011.01.012.
20. Jeziórska, R.; Świerz-Motysia, B.; Szadkowska, A.; Studziński, M.; Dzierżawski, J.; Kolasa, J.; Leszczyńska, I. Pol. Pat. Appl P-388 130, May 27, 2009.
21. Jeziórska, R.; Świerz-Motysia, B.; Szadkowska, A. Polimery 2010, 55, 748.
22. Jeziórska, R.; Świerz-Motysia, B.; Zielecka, M.; Szadkowska, A.; Dzierżawski, J.; Studziński, M.; Kolasa, J.; Komornicki, R.; Wartyni, M. Pol. Pat. Appl. P-391 875, July 19, 2010.
23. Jeziórska, R. Int Polym Process 2007, 22, 122.
24. Zapata, P.; Quijada, R.; Benavente, R. J Appl Polym Sci 2011, 119, 1771.
25. Benavente, R.; Perez, E.; Yazdani-Pedram, M.; Quijada, R. Polymer 2002, 43, 6821.
26. Nitta, K. H.; Tanaka, A. Polymer 2001, 42, 1219.
27. Jordens, K.; Wilkes, G. L.; Janzen, J.; Rohlfing, D. C.; Welch, M. B. Polymer 2000, 41, 7175.
28. Popli, R.; Glotin, M.; Mandelkern, L. J Polym Sci Part B: Polym Phys 1984, 22, 407.
29. Sinnott, K. M. J Polym Sci Part B: Polym Phys 1965, 3, 945.
30. Clas, S. D.; McFaddin, D. F.; Russell, K. E. J Polym Sci Part B: Poly Phys 1987, 25, 1057.
31. Cerrada, M. L.; Benavente, R.; Perez, E. Macromol Chem Phys 2001, 202, 2686.
32. Popli, R.; Mandelkern, L. Polym Bull 1983, 9, 260.